Distribution of α-Actinin in Single Isolated Smooth Muscle Cells

F. S. FAY, K. FUJIWARA, D. D. REES, and K. E. FOGARTY
Department of Physiology, University of Massachusetts Medical School, Worcester, Massachusetts 01605; and Department of Anatomy, Harvard Medical School, Boston, Massachusetts 02115

ABSTRACT In order to probe the organization of the contractile machinery in smooth muscle, we have studied the distribution of α-actinin, a protein present in high concentration in dense bodies, structures apparently analogous to the Z-disks of striated muscle. Localization of α-actinin in single isolated smooth muscle cells of the stomach muscularis of *Bufo marinus* was determined by analysis of the pattern of anti-α-actinin staining in single fluorescence photomicrographs, stereo pair micrographs, and computerized three-dimensional reconstructions from multiple image planes. The distribution of anti-α-actinin and antitubulin staining was compared in contracted and relaxed cells. The studies revealed that α-actinin is present in high concentrations in fusiform elements (mean axial ratio = 4.82) throughout the cytoplasm and in larger, more irregularly shaped plaques along the cell margins. Many of the fusiform-stained elements are organized into stringlike arrays characterized by a regular repeating pattern (mean center-to-center interspace = 2.2 ± 0.1 μm). These linear arrays appear to terminate at the anti-α-actinin stained larger plaques along the cell margin; several of these strings often run in parallel with their elements in lateral register. While this general pattern of organization is maintained in cells during contraction, the distance between successive stained elements in stringlike arrays is decreased. We suggest that the decrease in the distance between elements in these strings results from shortening of materials that constitute these linear arrays. We do not believe that the shortening within these arrays reflects compression by forces generated elsewhere within the cell, as the reorganization of noncontractile microtubules is qualitatively different from the changes in the pattern of anti-α-actinin staining.

It has generally been assumed that contraction in smooth muscle, as in striated muscle, is a consequence of the sliding of arrays of two filament types, one containing actin, the other myosin (11). Actin within smooth muscle is organized into filaments 6–8 nm in diameter (25), while myosin reportedly exists as filaments 12–15 nm in diameter (5, 6). The manner in which these filaments are arranged with respect to one another to produce force in smooth muscle is largely unknown. Several lines of evidence, however, suggest that thick and thin filaments may be organized into contractile fibrils that run for relatively short distances attaching at both ends to points along the cell membrane, the plasma membrane dense bodies. (*a*) Ultrastructural studies show that plasma membrane dense bodies appear to be the site of termination of thin filaments (23) and that during active shortening, the plasma membrane forms evaginations only in regions devoid of plasma membrane dense bodies (8). (*b*) Following permeabilization of single isolated smooth muscle cells, polarization optics reveal birefringent fibrils that run between points on the cell membrane and become more obliquely oriented as these cells contract (27, 28). (*c*) While such fibrils have not been seen in isolated living smooth muscle cells, such cells do show strong positive birefringence when relaxed; during active contraction, this birefringence is lost while negative birefringence becomes predominant (15). (*d*) Electron micrographs of single isolated smooth muscle cells show thick and thin filaments and dense bodies within the cytozone that in relaxed cells are oriented generally parallel to the long axis of the cell and are more obliquely oriented in contracted cells (7). While all of these data can be explained if the contractile proteins in smooth muscle are organized into contractile fibrils that run for relatively short distances between dense bodies on the plasma membrane (8), such fibrils have

THE JOURNAL OF CELL BIOLOGY · VOLUME 96 MARCH 1983 783–795

never been visualized within the intact smooth muscle cell.

The studies described in this report are aimed at probing further for the existence of such contractile elements. We reasoned that these contractile fibrils must be at least 35 μm in length, assuming that the relaxed smooth muscle cell is on the average 6 μm in diameter and that no structural elements that might constitute such fibrils are inclined more steeply than 10° relative to the long axis of the cell.[1] If these contractile fibrils are in turn composed of interdigitating arrays of thick and thin filaments whose length is generally comparable to that in skeletal muscle, then such fibrils must be composed of several sarcomerelike units of interacting thick and thin filaments organized in a series manner. Since cytoplasmic dense bodies appear to act much like Z-disks of striated muscle collimating thin filaments (1), the boundaries of these repeating sarcomerelike units ought to be marked by these dense bodies. Immunocytochemical studies by Schollmeyer et al. (26) have indicated that the dense bodies of smooth muscle contain α-actinin, as do the Z-disks of striated muscle. Thus we utilized antibodies against this protein to search for the existence of contractile fibrils within single isolated smooth muscle cells.

Several studies using immunofluorescence to investigate the distribution of putative contractile proteins in smooth muscle have appeared over the past few years (2, 3, 18, 19). The earliest studies reported that in cultured cells derived from smooth muscle the pattern of antimyosin staining was striated and revealed widespread order (19), but the authors themselves indicated that the pattern observed might be an aggregation artefact. More recently, Bagby and Pepe (3), concerned about possible changes in smooth muscle cells in culture used in earlier studies, investigated the pattern of antimyosin staining in glycerinated smooth muscle cells freshly isolated from the chicken gizzard. While distinct patterns of staining within whole cells were only faintly detectable, in broken cells myofibrillike structures with a periodic antimyosin staining pattern were clearly observed. During the course of the present study, Bagby (2) reported on anti-α-actinin staining again in glycerinated chicken gizzard cells. Membrane-associated α-actinin-containing structures were clearly seen, but only faint discrete staining within the cytoplasm, principally adjacent to the cell membrane, was evident.

The studies described in this paper were carried out on smooth muscle cells fixed before cell permeabilization and antibody staining to minimize movements of the contractile proteins during preparation for immunocytochemistry. Numerous discrete α-actinin-containing structures within the cytoplasm are revealed by analysis of the pattern of anti-α-actinin staining. These elements are organized into arrays whose dimensions are altered upon contraction in a manner suggesting that they themselves are part of the contractile apparatus.

MATERIALS AND METHODS

Isolated Smooth Muscle Cells: Suspensions of single isolated smooth muscle cells were obtained by enzymatic disaggregation of thin slices of stomach muscularis of the toad, *Bufo marinus*, by methods previously reported (10). Briefly, thin tissue slices were incubated in collagenase (1 mg/ml; Sigma, Type I, Sigma Chemical Co., St. Louis, MO) and trypsin (1 mg/ml; Sigma Chemical Co., Type III) for 30 min at 30°C, followed by three serial incubations of 45 min each in collagenase (0.5 mg/ml) alone. The smooth muscle cells used in these studies were obtained during the second and third incubations with collagenase and were studied between the second and sixth hour after isolation.

Antibodies: Rabbit antibodies against chicken gizzard α-actinin (14), toad stomach α-actinin, and sea urchin egg tubulin (13) were used. α-Actinin from toad stomach was purified (Fig. 1 *a*) by methods described in abstract form to date (24). Antibodies against toad α-actinin were raised as described (13). Both rabbit anti-chicken gizzard α-actinin and rabbit anti-toad stomach α-actinin were specific for α-actinin amongst proteins in a homogenate of toad stomach muscularis as revealed by immunoelectrophoresis (Fig. 1 *b*) performed as described (13). The patterns of anti-α-actinin staining were identical with rabbit anti-toad α-actinin and anti-chicken α-actinin. Rhodamine-labeled goat anti-rabbit IgG was obtained from Cappel (Cappel Laboratories, Cochranville, PA).

Antibody Staining: The suspensions of smooth muscle cells in amphibian physiological saline (10) were pipetted onto glass coverslips previously coated with polylysine by dipping them in 0.1% polylysine in H_2O for 5 min and air-drying them. The cells were allowed to settle for 2 h. Some smooth muscle cells were induced to contract by adding to each coverslip acetylcholine in amphibian physiological saline to a final concentration of 10^{-4} M for 1 min before fixation (12).

Cells were fixed for 10 min at room temperature with 3.7% formaldehyde in amphibian physiological saline (10). The coverslips were washed for 10 min in phosphate-buffered saline [PBS (14)] and were immersed for 10 min into acetone (−20°C) or PBS containing 0.05% Triton X-100 (0°C) in order to permeabilize cells. Coverslips treated with acetone were then allowed to air-dry; those treated with Triton X-100 were washed for 10 min with PBS. In all subsequent steps, the coverslips were treated identically, and since cells permeabilized by the two procedures gave identical results the method of membrane permeabilization will not be indicated for each experiment.

Cells were then treated with 60 μl of fluorescently labeled anti-α-actinin (240 μg/ml IgG; dye to protein ratio = 1.8–2.5) or unlabeled antitubulin (serum diluted 100× with PBS) at 37°C for 30 min, 1 h, or 2 h. The 1-h incubation routinely yielded the most detailed patterns of staining with the lowest background. After several PBS washes, antitubulin-stained cells were treated with rhodamine-labeled goat anti-rabbit IgG (100 μg/ml); for 30 min at 37°C. Controls for the specificity of anti-α-actinin staining were: (*a*) to stain cells with labeled anti-α-actinin absorbed with purified α-actinin, or; (*b*) to stain cells with preimmune serum. The absorbed anti-α-actinin was prepared by incubating at 4°C for 2 d labeled antibodies with acetone-precipitated and formaldehyde-fixed α-actinin isolated from chicken gizzard. The resulting immune complex was removed by centrifugation at 12,000 *g* for 15 min. Fluorescently labeled cells were mounted in 50% glycerol in PBS.

Fluorescence Microscopy: Both a Zeiss inverted microscope (ICM 35) and Leitz Orthoplan microscope equipped with an epi-illumination attachment were used. All observations were made using either a Zeiss planapo 63× (NA = 1.4, oil) or 100× (NA = 1.3, oil) objective lens. The fluorescent images were recorded on either Kodak SO-115 or Kodak Tri-X film. These films were

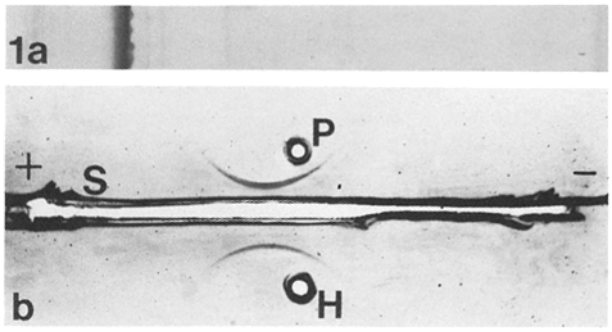

FIGURE 1 (*a*) 10% SDS polyacrylamide gel according to Laemmli (20) of α-actinin purified from toad stomach muscularis. 10 μg applied to the gel, which was allowed to migrate at constant power (10 W) for 6 h. Protein was assessed by Coomassie-Blue staining. Densitometric scans revealed that the integrated optical density associated with the α-actinin peak was 90% of the total, and that remaining stained material was distributed over seven minor bands. (*b*) Immunoelectrophoresis plate stained with Coomassie Blue. Anti-toad α-actinin was applied to the trough, and purified toad α-actinin (*P*) to the top well and a crude homogenate of toad stomach (*H*) to the bottom well. Note that the anti-α-actinin forms a single precipitin band with both purified α-actinin and whole homogenate.

[1] The estimate of maximum contractile element angle is derived from measurements from electron micrographs of thick filament and dense body orientation in longitudinal sections of relaxed single smooth cells, which revealed a range of angles for the long axis of both structures relative to that of the cell of 0–10° (F. S. Fay, unpublished observation).

developed with Kodak D-19 or Ethol developer (Ethol Chemicals Inc., Chicago, IL) to an effective ASA of 100 and 1000, respectively. Fluorescence stereo micrographs were taken according to the method of Osborn et al. (22).

Analysis of the Fluorescent Image: To obtain information regarding the three-dimensional organization of fluorescently labeled α-actinin containing bodies, we obtained multiple fluorescence photomicrographs of a cell at 0.5-μm intervals by shifting focal planes. In order to obtain photomicrographs at focal planes that were spaced apart by a known amount, the microscope was modified so that the distance between the objective lens and the specimen could be rapidly determined with a high degree of precision. For this purpose, the nosepiece of the microscope was modified (Fig. 2*a*) to hold an eddy current sensor (Kaman Measuring Systems, Kaman Sciences Corp., Colorado Springs, CO, Model KD 2300-.5 SU). This device produces an output voltage that is linearly related to the distance between the tip of the sensor and the underside of the stage with a sensitivity of 36 mV/μm (Fig. 2*b*). The noise on the sensor's output is never greater than 1 mV, resulting in a resolution of lens displacement of at least 0.03 μm. As shown in Fig. 2*c*, a displacement of 0.5 μm could easily be detected in the output of the Eddy current sensor. A given position of the stage could be maintained within the resolution of this detector for greater than 30 s, more than sufficient to obtain a picture with Tri-X film. A typical relaxed cell required ~14 successive images to fully record the distribution of fluorescence.

Because the small fluorescently stained bodies containing α-actinin were found to produce a recognizable image over a 2-μm range of focus, it was necessary to devise the method shown in Fig. 3 to determine the true positions of all the fluorescent bodies in the cell. Successive fluorescence photomicrographs of a single smooth muscle cell were obtained at specimen planes ~0.5 μm apart. Transparencies containing tracings of all the stained bodies in a series of photomicrographs were stacked and aligned using features of the field outside the cell or large fluorescent bodies within the cell as reference points. The aligned transparencies were placed on a light box and scanned for vertically aligned consecutive fluorescent bodies of roughly comparable size. When such a cluster spanned an odd number of image planes, we concluded that the stained body existed within the cell in the plane corresponding to the middle image plane. When such a cluster spanned an even number of planes, we flipped a coin to decide to which of the two middle planes the structure should be assigned. Fluorescent spots with no corresponding ones in the adjoining transparencies were eliminated. The assignment of a structure to a given plane was designated by intensifying the tracing of it on the transparency corresponding to the specimen plane to which it was assigned.

Computer Reconstruction of Fluorescent Body Distribution: In order to assess the three-dimensional distribution of fluorescent bodies within a smooth muscle cell, information present on the transparencies

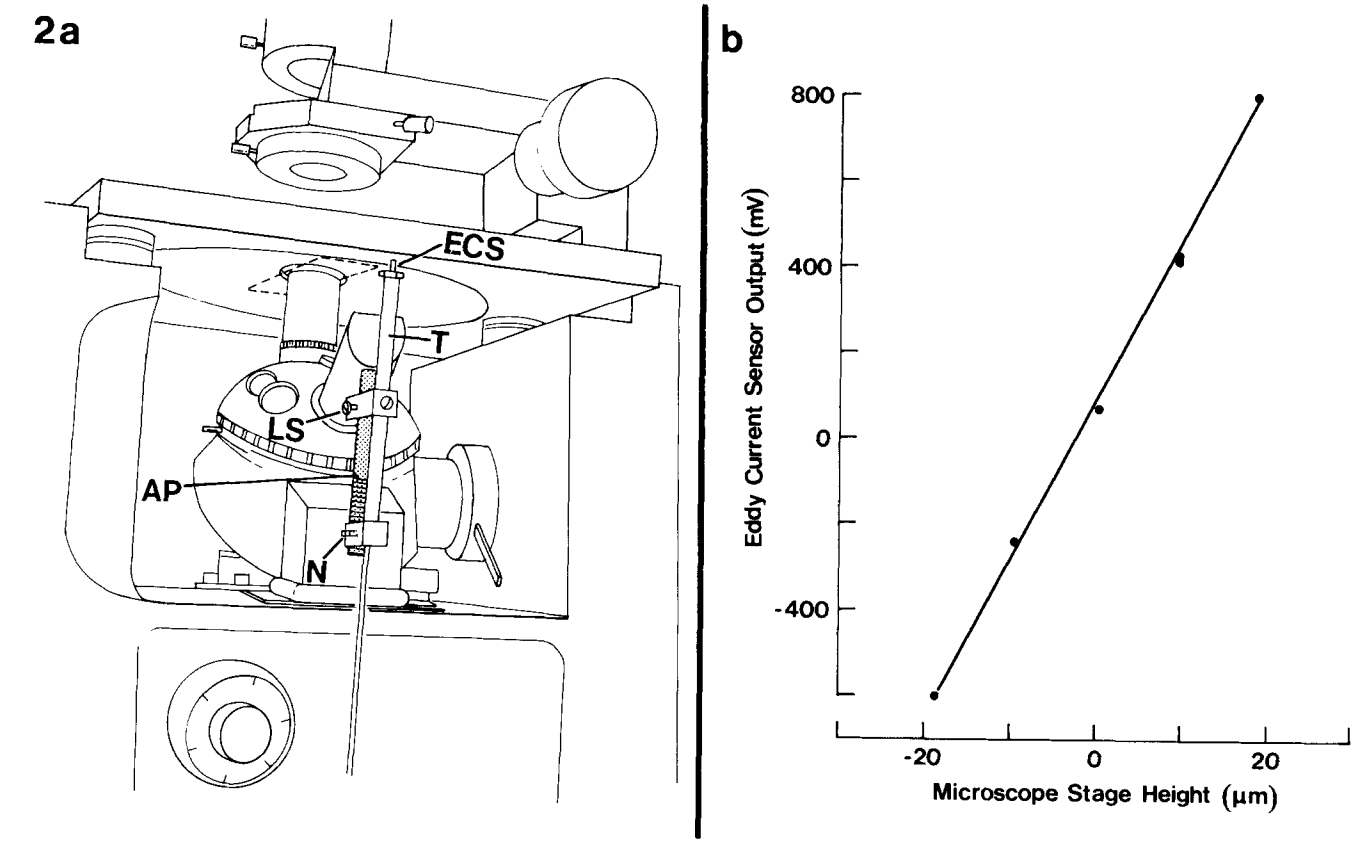

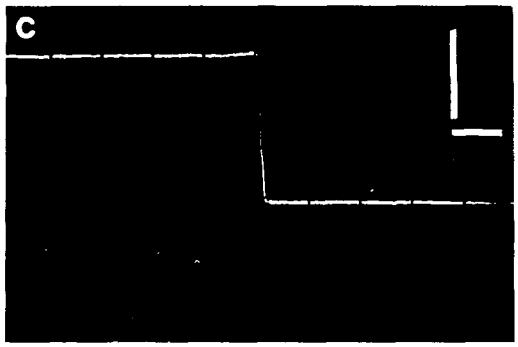

FIGURE 2 (*a*) Schematic illustration of modification of fluorescence microscope to assess distance between microscope objective and specimen. An eddy current sensor (*ECS*) was mounted in a brass tube (*T*) which was attached to the nosepiece of the microscope. The position of the vertically mounted tube relative to the underside of the microscope stage could be adjusted by turning the nut (*N*) on the stainless steel alignment post (*AP*). The vertical tube was positioned at the start of each day using the nut so that the ECS gave no output when a specimen was approximately in focus, and the position of the tube was then locked by tightening the locking screw (*LS*). The ECS electronics come adjusted from the factory so that zero output is achieved when the distance between the ECS tip surface and a metal target is 125 μm. (*b*) Output voltage of the eddy current sensor vs. changes in distance between the nosepiece and stage of the microscope. Changes in the position of the nosepiece were detected by coupling it to a Starrett dial test indicator (L. S. Starrett Co., Athol, MA). Note that the eddy current sensor had a sensitivity of 36 mV/μm. (*c*) Oscilloscope recording of eddy current sensor output during a change in microscope focus of 0.5 μm. Note that output noise is virtually nondetectable at this recording sensitivity and that the new focus level is maintained for the duration of this recording. Vertical bar, 10 mV; horizontal bar, 1 s.

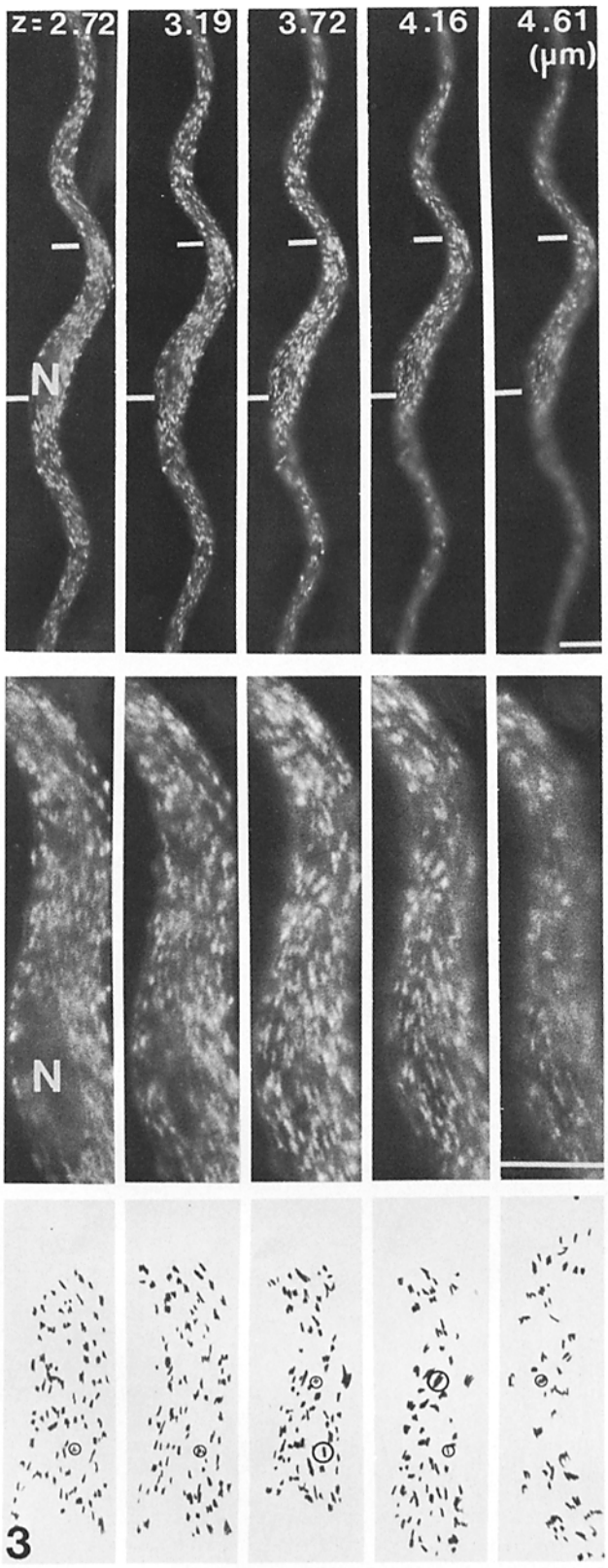

FIGURE 3 Five fluorescence photomicrographs of a single smooth muscle cell stained with anti-α-actinin. *Top Row.* Shows image of entire length of the cell obtained at five different focal planes spaced ~0.5 μm apart. Changes in focal plane were measured as described in Fig. 2 and are expressed relative to the plane where the image of the bottom surface of this cell just went out of focus, which was assigned a Z-axis position of 0. Note that the area devoid of stain is occupied by the nucleus (*N*) as revealed by Nomarski optics. *Middle Row.* Enlargement of the portion between the white darts of each of the fluorescence photomicrographs in the row above. *Bottom Row.* Tracings of the size and position of the stained elements in a portion of the photomicrographs in the row above. When these tracings on transparent plastic were stacked vertically and aligned as described in the text, many of the fluorescently stained elements appeared in several successive tracings. Two such stained elements have been circled in the planes where they successively appear. The image corresponding to the focal plane in which, in reality, each of these two elements is situated is indicated by the larger circle pair. In this and all other photomicrographs, the calibration bar indicates 10 μm unless otherwise specified.

regarding the size, position and orientation of individual fluorescent bodies in sequential 0.5-μm specimen planes was entered into a DEC 11/40 (Digital Equipment Corp., Marlboro, MA) computer using a Hi-Pad X, Y-digitizer (Houston Instruments, Austin, TX). Fluorescent bodies that were <0.3 μm wide were represented as a single vector, whereas larger fluorescent bodies found principally along the plasma membrane were represented as a pair of crossed vectors with the coordinates of the beginning and end of each vector marking one of four extreme vertices of the body. The resulting three-dimensional matrix was displayed on a GT-40 graphics terminal (Digital Equipment Corp.) statically or dynamically by rotating the image around an axis. Stereo views of the reconstructions were obtained by photographing the display on the GT-40 terminal with the matrix rotated ± 6° of the perspective desired. Portions of the display were intensified utilizing a light pen associated with the GT-40 under control by a subroutine in the display program.

RESULTS

The pattern of anti-α-actinin staining in a typical relaxed single smooth muscle cell is shown in Fig. 4*a* and *b*. The structures stained by anti-α-actinin are of two general classes. The largest and most intensely stained structures are usually found along the periphery of the cell, presumably in association with the plasma membrane. These structures are more irregular in shape and less numerous than those found in the inner regions of the cell, which are fusiform in shape. The region occupied by the nucleus (*N*) is devoid of anti-α-actinin staining. The staining was specific for α-actinin as demonstrated by the results of several controls described in Materials and Methods. For example, no fluorescent staining was detected when cells were incubated under conditions identical to those used for Fig. 4*a* and *b* with anti-α-actinin preabsorbed with α-actinin (Fig. 4*c* and *d*).

Several higher power views of an inner region of a single smooth muscle cell in Fig. 5 show the characteristic size and shape of the structures stained by anti-α-actinin. The mean axial ratio of the fusiform-stained structures in relaxed smooth muscle cells is 4.82 ± 0.15; their mean length is 1.25 ± 0.10 μm. They are clearly within the cytoplasm and not associated with the membrane. This localization is evident from inspection of Fig. 5*c* where stained fusiform structures are in the plane containing the nuclear void (*N*) and where the larger stained patches (large white arrows) that characterize the surface of the cell are clearly absent except along the periphery of the cell's image. Similar conclusions may be reached by inspection either of the computer reconstructions of the distribution of these anti-α-actinin-stained bodies (Fig. 6) or of stereo pair photomicrographs (Fig. 7).

The fluorescence photomicrographs suggest that these stained bodies are organized into strings. The stained bodies in such strings characteristically have their long axis subtending the same solid angle relative to the long axis of the cell as the one preceding it. In addition, the center-to-center distance between stained elements in such strings is quite regular as seen in Fig. 8*a* and *c* (open triangles). Because of the large

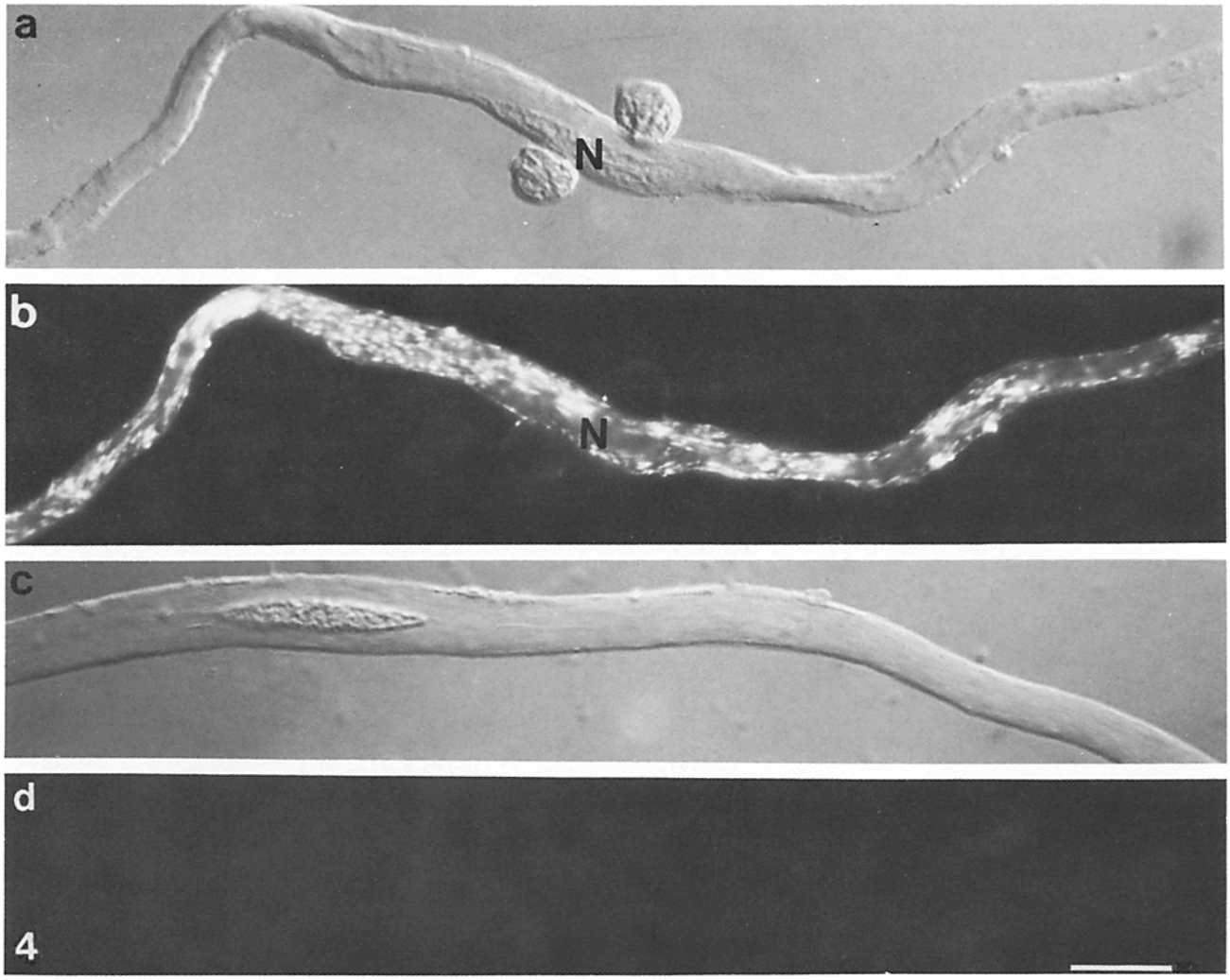

FIGURE 4 (*a* and *b*) Nomarski (*a*) and fluorescence (*b*) images of a single smooth muscle cell stained with anti-α-actinin. Both fluorescence and Nomarski images were obtained at the same focal plane. Note that the region occupied by the nucleus (*N*) is devoid of fluorescently stained elements. (*c* and *d*) Nomarski (*c*) and fluorescence (*d*) images of a single smooth muscle from the same cell suspension as in *a* and *b*, subject to identical staining protocols with anti-α-actinin preabsorbed with α-actinin, and photographed under identical conditions. Note the absence of fluorescent staining in *d*.

depth of focus associated with such fluorescence images, the possibility must be considered that α-actinin-stained bodies that appear to be in a stringlike array are in fact in quite different planes. This does not appear to be the case, however, as judged from images where the Z-axis uncertainty has been reduced by obtaining stereo pair images or by viewing computer reconstructions. Fig. 7 shows two stereo pairs of a single smooth muscle cell where stained elements within the cytoplasm are arranged in a stringlike manner as suggested by a single fluorescence image. Such strings are even more strikingly evident from inspection of the computer reconstructions of the distribution of fluorescence within a portion (~50 μm length) of a single smooth muscle cell (Fig. 6). The stereo pairs of these reconstructed images clearly indicate that the strings do not reflect superposition of structures from widely different planes within the cell onto a single image plane.

In both single fluorescence photomicrographs (Fig. 5) and the computer reconstruction (Fig. 6), areas can be found where strings of stained elements (Fig. 5 *a*, *b*, and *c*; solid triangles) appear to head towards the large stained elements (large arrows) along the membrane where they terminate. Several strings of stained elements are occasionally observed to run in parallel for some distance. The individual stained elements constituting such strings are often in register laterally (Fig. 5 *b*, *c*, and *d*; small arrows). The computer reconstruction also reveals regions where elements in several strings that appear to run in parallel are in register laterally for two or more cycles (Fig. 6). In these regions, the stained elements appear to be more closely spaced than in regions of the cell where adjacent stained elements are not so registered. The linear arrays of stained elements are quite similar to the contractile fibrils that we had inferred existed from earlier studies.

To test whether these linear arrays may indeed be contractile, we compared the distribution of anti-α-actinin stained elements in cells fixed in the relaxed state with ones fixed during contraction. Fig. 8 shows fluorescence and Nomarski photomicrographs of a single cell fixed after exposure for 60 s to 10^{-4} M acetylcholine. The Nomarski image of this fixed cell reveals that its surface membrane is highly evaginated and that its nucleus is compressed and folded, a pattern consistently

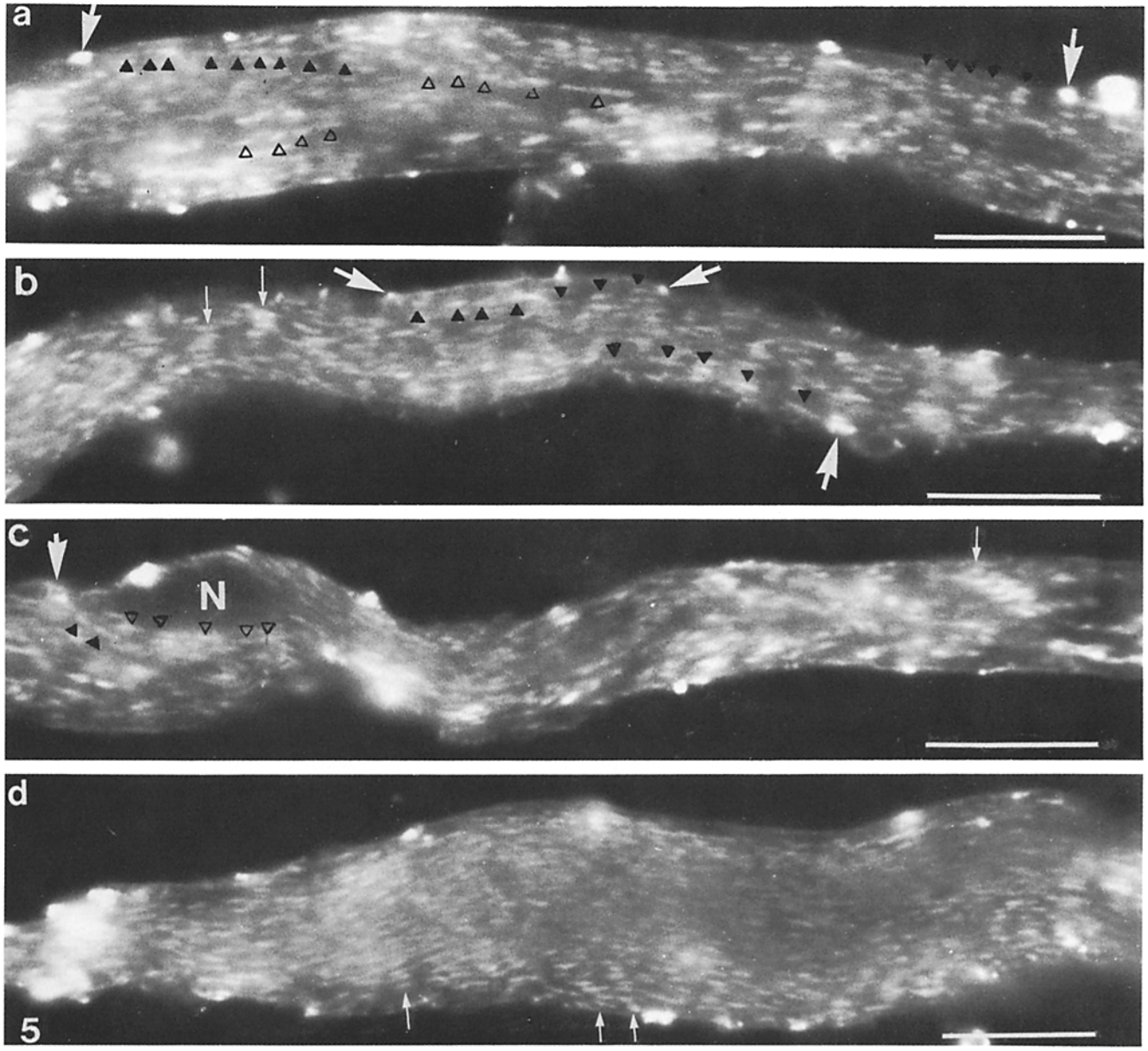

FIGURE 5 High magnification fluorescence photomicrographs of four smooth muscle cells stained with anti-α-actinin. Note that the fusiform-stained elements are found throughout the cytoplasm. The region occupied by the nucleus in *c* is devoid of stain whereas numerous fusiform-stained elements are found within this focal plane. The larger more irregular stained elements (large white arrows) are confined to the outer margins in this and other images (Fig. 8 *a*, *b*, and *d*) when the microscope was focused midway along the depth of the cell. Several of the fusiform-stained elements within the cytoplasm appear to be part of a stringlike array (open triangles) characterized by a relatively regular spacing between stained elements. In several regions, the strings of fusiform-stained elements appear to run in parallel for some distance with stained elements in lateral register (small arrows). Some of these strings (solid triangles) appear to terminate at the larger plaques stained by anti-α-actinin along the cell margins (large arrows). Nuclear void (*N*) is apparent.

FIGURE 6 Four stereo pairs of a computer reconstruction of the distribution of anti-α-actinin-stained elements within a portion of a single isolated smooth muscle cell. (*a* and *a'*) Two views of the distribution of anti-α-actinin staining. The three-dimensional matrix was rotated by 12° in *a'* relative to *a*. Note that the ellipsoidal region devoid of stain within this cell was occupied by the nucleus. The fusiform-stained elements within the cytoplasm are represented as single vectors and the larger plaques along the cell periphery as cross vectors as described in the text. Note that the fusiform-stained elements represented by single vectors run generally parallel to the long axis of this relaxed cell. (*b* and *b'*) Same as the preceding stereo pair in which six of the stained elements which appear to run in a stringlike array have been intensified relative to the other elements (arrow, *b'*). Other such strings can also be identified within this reconstruction. (*c* and *c'*) Same as the preceding stereo pair in which seven stained elements within the cytoplasm have been intensified. These seven are part of two groups (arrows, *c'*) of laterally close-spaced and in-register elements. The two groups are denoted by lateral connections between nearest neighbors. Note that several of the elements in these two groups appear to be part of stringlike arrays. (*d* and *d'*) Same as preceding stereo pairs in which two of the larger stained elements along the cell periphery denoted by crossed vectors (arrows, *d'*) have been intensified. Several fusiform elements that are part of two stringlike arrays that appear to terminate at these larger plaques have also been intensified. × 2,370.

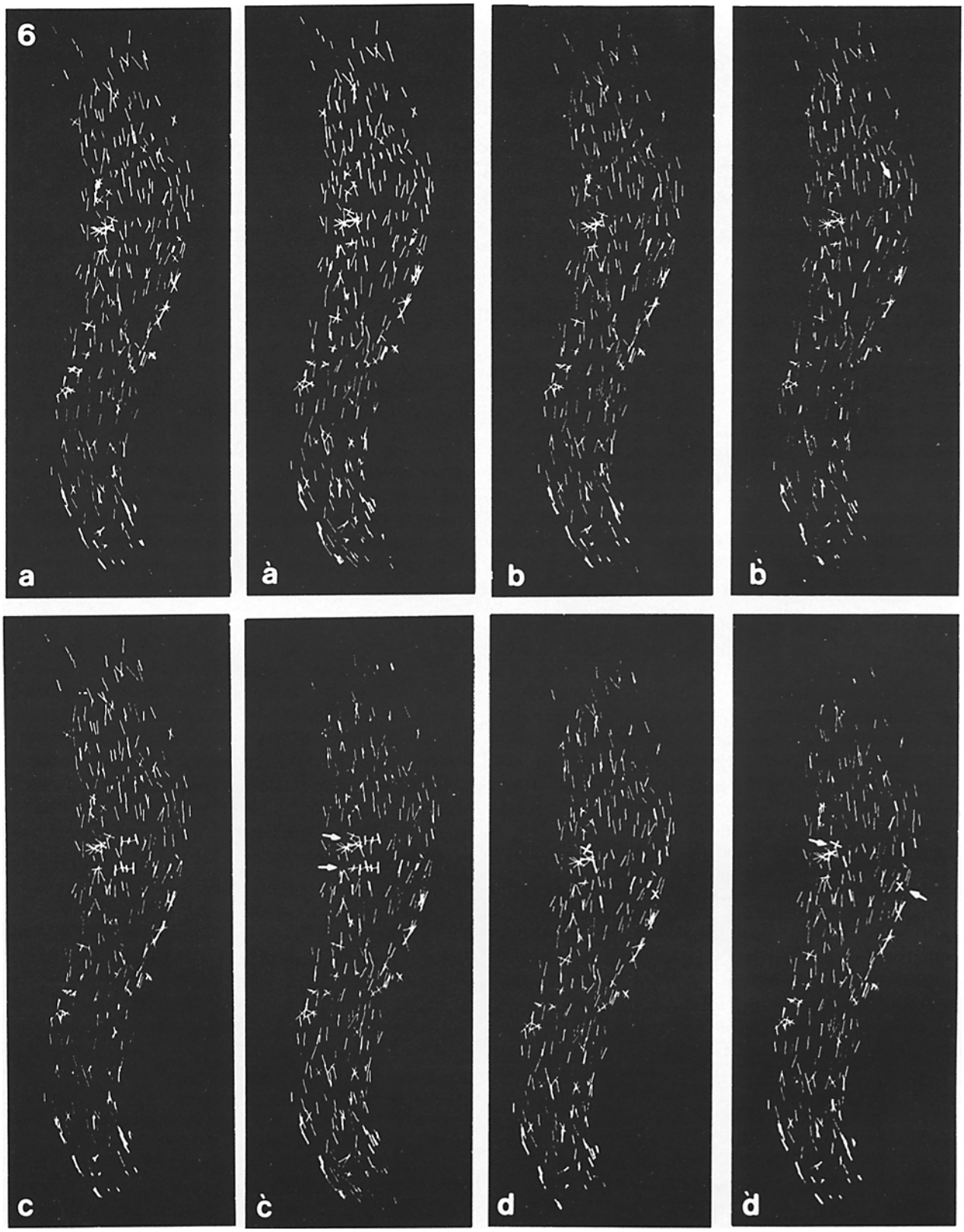
6
a
à
b
ḃ
c
ċ
d
ḋ

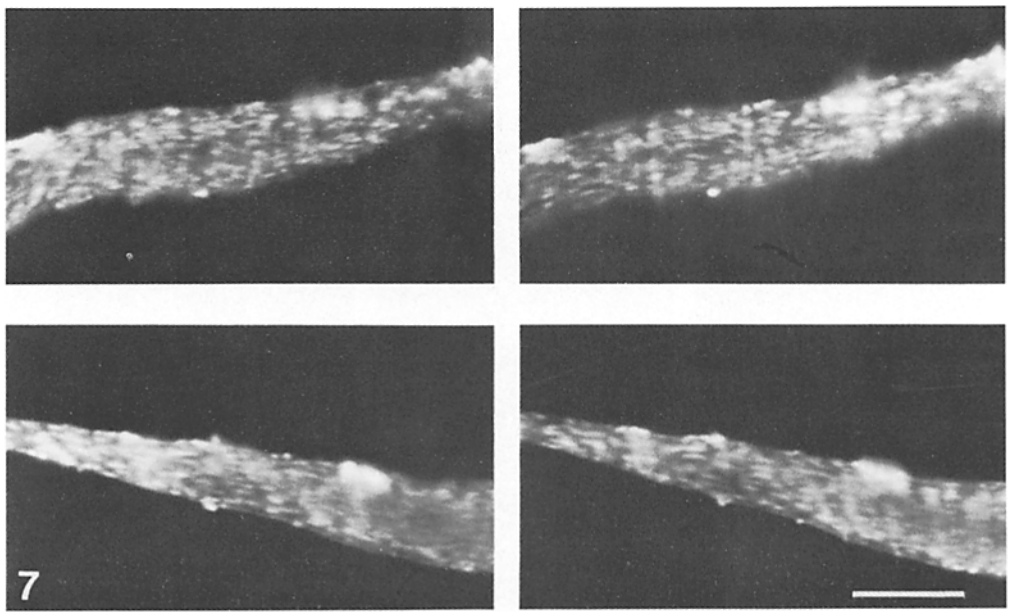

FIGURE 7 Stereo pair fluorescence photomicrographs of two smooth muscle cells stained with anti-α-actinin. Note the stringlike arrays of stained fusiform elements in the cytozone. In several regions, elements in adjacent strings are in lateral register.

seen in living cells observed with Nomarski optics during active cell shortening. The pattern of fluorescent anti-α-actinin staining in this contracted cell is, in a number of features, similar to that seen in relaxed cells. Two classes of stained structures are observed. Within the cell, fusiform stained elements are seen, whereas along the cell margins larger, more irregularly shaped, stained structures are evident (large arrows). The stained fusiform elements within the cytoplasm of contracted cells are on average shorter and wider than those seen in relaxed cells. For example, in the contracted cell in Fig. 8, the mean axial ratio of fusiform stained elements is 1.87 ± .09 (SE, n = 16), in comparison to a mean axial ratio of 4.82 ± 0.15 (SE, n = 28) measured in several relaxed cells. In single fluorescence photomicrographs of contracted cells, the stained fusiform elements are observed to run in stringlike arrays within the cytoplasm (Fig. 8, triangles) often at a slightly steeper angle than seen in relaxed cells. As in relaxed cells, lateral registration of anti-α-actinin-stained elements is evident in the contracted cell shown in Fig. 8 (small arrows). These features are also evident in the three-dimensional reconstruction of the distribution of anti-α-actinin-stained elements within a contracted cell (Fig. 9). The fusiform-stained elements are clearly shorter and are inclined somewhat more steeply than those seen in the relaxed cell in Fig. 6. There are areas within this reconstruction where stained elements are organized in a stringlike array (Fig. 9 *b*) apparently terminating at a larger anti-α-actinin-stained plaque along the periphery. Lateral registration of the stained elements within the cytozone is also evident in some regions (Fig. 9 *b*). The larger stained elements along the cell margins appear to be found in areas that correspond to the bases of evaginations seen with Nomarski optics (Fig. 10). A definitive assessment of the position of the large anti-α-actinin-stained areas along the membrane and the pattern of membrane evaginations is complicated by the large depth of focus associated with the fluorescent images and thus must await three-dimensional reconstruction of both the fluorescence and Nomarski images.

The center-to-center distance between sequential elements in these strings appears to be decreased relative to relaxed cells. In order to evaluate the extent of such shortening, we measured the distance between midpoints of successive stained elements in linear arrays in the computer reconstructions. Such measurements were only made between stained elements in linear arrays assigned to a single optical plane, in order to minimize uncertainties in the measurement of distances between stained elements in linear arrays that might be introduced by the projection of an array tilted steeply relative to the plane of view. Fig. 11 *a* shows a single optical plane, in a relaxed smooth muscle cell used for the computer reconstruction, which shows three linear arrays of stained elements. The distance between the midpoints of the six pairs of stained elements ranged from 1.77 to 2.78 μm. The mean distance between midpoints of 37 such pairs in two relaxed cells was 2.2 ± 0.1 (SE) μm. In the one contracted cell reconstructed by these means to date, several of the optical planes contained linear arrays; Fig. 11 *b* shows two such linear arrays, with distances between successive stained elements of 1.27 and 1.36 μm. The mean distance between 22 such pairs in this contracted cell was 1.4 ± 0.1 (SE) μm. The frequency distributions of distances between stained elements in such linear arrays in both relaxed and contracted cells are compared in Fig. 12. In relaxed cells the distances between such elements ranged from 3.3 to 1.2 μm; in the contracted cell the distance decreased, ranging from 2.4 to 0.6 μm.

The observation that the distance between anti-α-actinin-stained elements in such linear arrays is diminished in cells that have actively shortened is consistent with the concept that these linear arrays are contractile structures. While this result might be interpreted as reflecting compression of these linear arrays by contraction elsewhere within the cytoplasm, this appears to be unlikely given the pattern of antitubulin vs. anti-α-actinin staining in both relaxed and contracted cells. Since much of the cellular tubulin exists as microtubules that are not contractile, their pattern of distribution should reflect how noncontractile structures are distorted by forces generated elsewhere within the cell. As can be seen, the pattern of antitubulin staining in relaxed smooth muscle cells (Fig. 13 *a* and *b*) reveals the existence of many fine fibrils running parallel to the long axis of the cell. These structures appear to originate from a region near the nucleus, presumably the microtubule organizing center seen in other cells. A punctate pattern of antitubulin

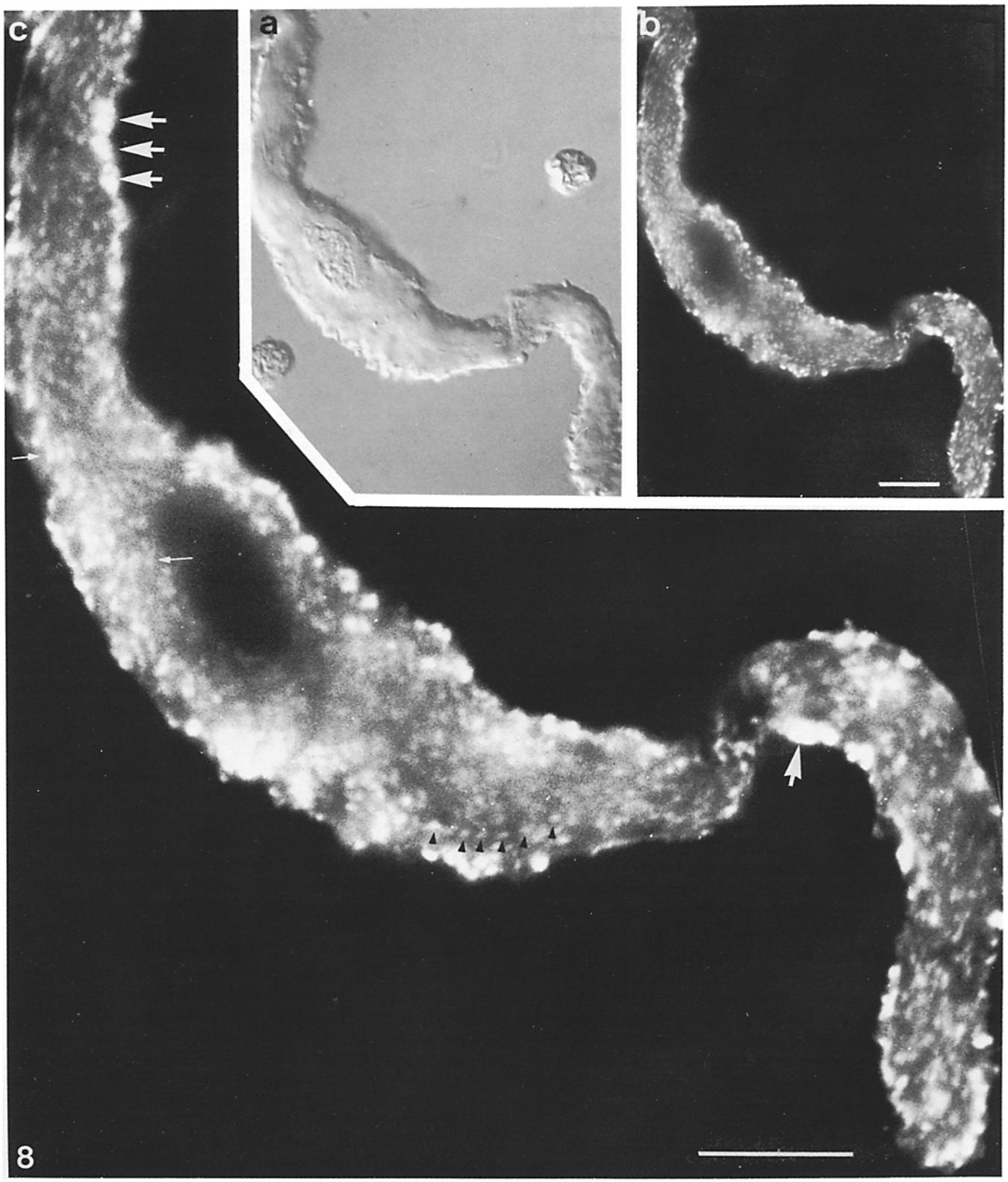

FIGURE 8 Fluorescence and Nomarski images of a single smooth muscle cell exposed to the contractile agonist acetylcholine (10^{-4} M) for 60 s before fixation. (*a*) Nomarski image of this cell showing numerous evaginations of the cell membrane and crenation of the nucleus, characteristic of living contracted single smooth muscle cells (8). (*b* and *c*) Fluorescence images of this cell at two different magnifications. Note that stringlike arrays of anti-α-actinin-stained elements (triangles) can be observed. Some of these strings appear to run in parallel for some distance with elements in lateral register (small arrows). Larger, more irregular anti-α-actinin-stained plaques along the cell margins are evident (large arrows), and some of the strings appear to terminate at these areas. Several of these stringlike arrays in this contracted cell appear to be more steeply inclined relative to the cell's long axis than in relaxed cells.

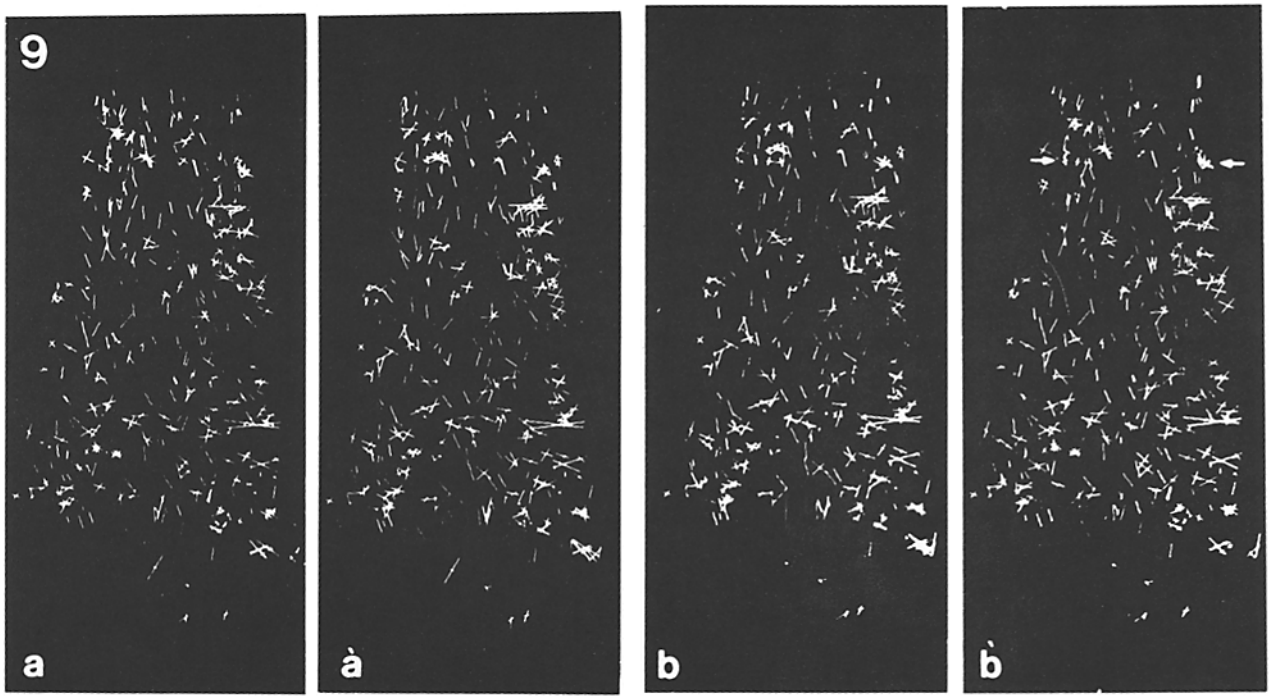

FIGURE 9 Two stereo pairs of a computer reconstruction of the distribution of anti-α-actinin-stained elements within a portion of a smooth muscle cell fixed in the contracted state. (*a* and *a'*) Stereo pair view of the distribution of the stained elements. (*b* and *b'*) Same as the preceding stereo pair in which three of the stained elements that appear to run in a stringlike array into a larger stained plaque along the cell periphery have been intensified relative to the other elements (arrow). Three of the stained elements that are part of a lateral group similar to that in Fig. 6 *c* and *c'* have also been intensified and interconnected (arrow). ×2,230.

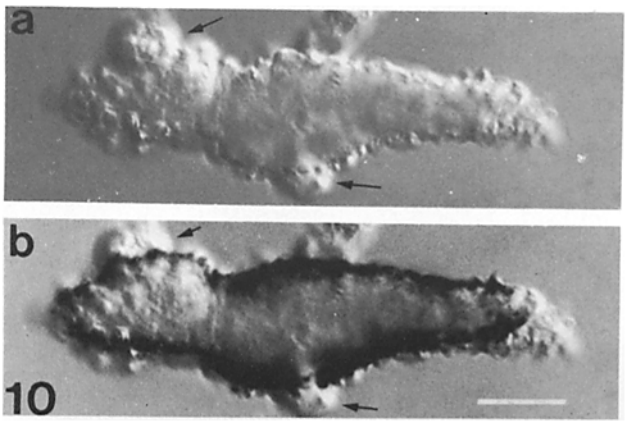

FIGURE 10 Fluorescence and Nomarski images of a single smooth muscle cell subject to a contractile stimulus as in Fig. 9 before fixation and staining with anti-α-actinin. The Nomarski and fluorescence images were obtained at the same focal plane. The fluorescence image was contrast reversed photographically and is superimposed on the Nomarski image in (*b*). Note the absence of anti-α-actinin staining along those portions of the membrane forming evaginations (arrows).

staining was observed within the nucleus. Near the microtubule organizing center a striking antitubulin-staining structure can be found which runs perpendicular to the long axis of the cell. This presumably is the primary cilium originally described in smooth muscle by Sorokin (29) using the electron microscope and described more recently by immunofluorescence in numerous cell types (e.g., reference 31). In contracted smooth muscle cells, microtubules are oriented more steeply relative to the long axis of the cell and are characterized by an undulating pattern (Fig. 13 *C*). While the linear arrays of anti-α-actinin-stained elements in contracted cells run more obliquely than in relaxed smooth muscle cells, they retain a linear organization (Figs. 8 and 9). Thus, the linear arrays of anti-α-actinin-stained elements and the antitubulin-stained fibers which have a similar course in relaxed cells appear to have quite different courses in a cell following contraction.

DISCUSSION

The present studies on single isolated smooth muscle cells have revealed that α-actinin appears to be concentrated in discrete structures both within the cytoplasm and along the margins of the cell. The staining pattern observed with fluorescently labeled anti-α-actinin has been shown to be specific for α-actinin. Furthermore, immunoelectrophoresis revealed that the anti-α-actinin used in the present studies was specific for α-actinin amongst proteins in the toad stomach muscularis. The protein purified from toad stomach that we call α-actinin is quite similar to α-actinins from other muscles (17, 30), as judged from its molecular weight—determined from SDS PAGE (mol wt = 100,000)—and its ability to increase the viscosity of striated muscle F-actin (24). Antisera prepared against chicken gizzard α-actinin cross-reacted with α-actinin from toad stomach, indicating immunologic similarities of α-actinins between these species.

The structural elements stained by anti-α-actinin within the interior of the cell and those along its margins most probably correspond, respectively, to the cytoplasmic and plasma membrane dense bodies observed with the electron microscope. The size (0.25 μm width; 1.25 μm length), ellipsoidal shape, and orientation (generally parallel to the long axis of the cell) of the internal structures stained by anti-α-actinin agree quite well with the reported dimensions (0.1–0.2 μm width, >1 μm

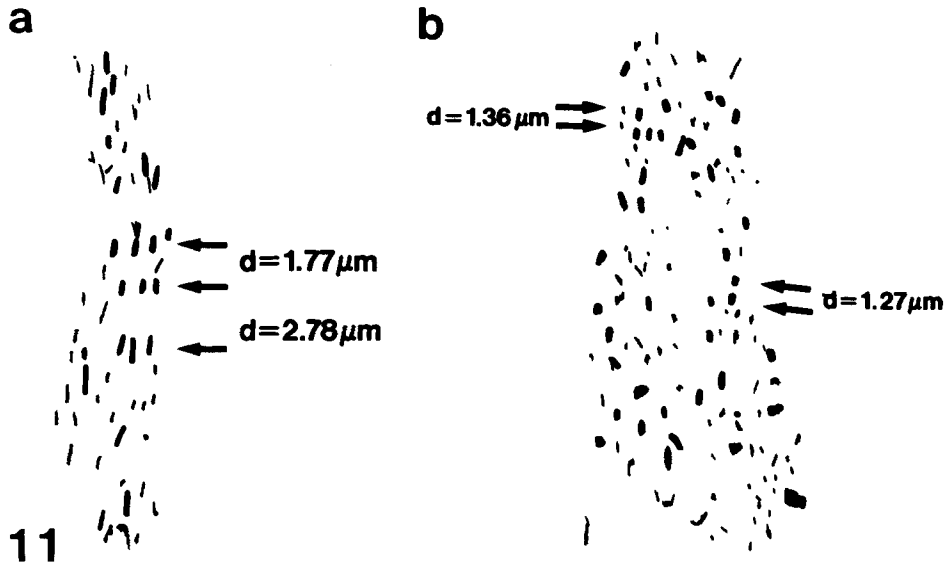

FIGURE 11 Tracings of the distribution of anti-α-actinin staining in a single optical plane of the relaxed (*a*) and contracted (*b*) smooth muscle cells shown in Figs. 6 and 11, respectively. The optical plane containing each of these stained elements was determined as described in the text and in Fig. 3. Those elements that exist in the cell in a plane corresponding to this image plane are denoted with a thickened tracing. Several of the stained elements that have been assigned to these two planes are part of stringlike arrays. Where pairs of stained elements comprising such strings have been assigned to this plane, the center-to-center distance between such pairs has been measured and is noted.

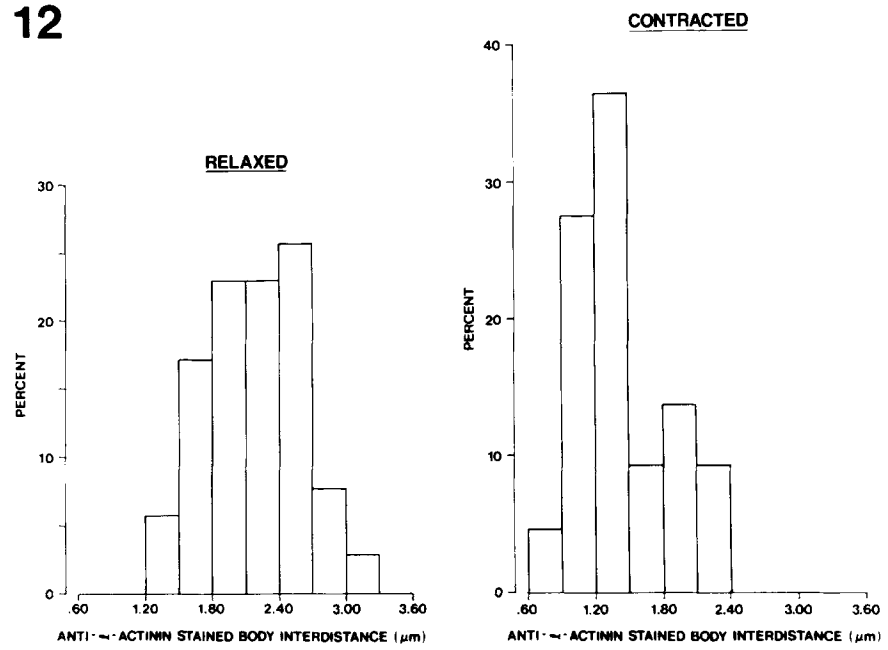

FIGURE 12 Histogram of the center-to-center distance between successive fusiform anti-α-actinin-stained elements in stringlike arrays within one contracted and two relaxed cells. The measurements were made as described in Fig. 12. Note the decrease in the distance between anti-α-actinin-stained elements in the contracted vs. relaxed cells.

long) and orientation of cytoplasmic dense bodies (16). The stained elements along the outer margins of the cells we believe correspond to the plasma membrane dense bodies observed in the electron microscope. We base this on the observation that when isolated smooth muscle cells contract, forming membrane evaginations, fluorescent anti-α-actinin staining is principally associated with the nonevaginated portions of the membrane, as are the plasma membrane dense bodies (7, 8). In both contracted and relaxed cells, the areas stained by anti-α-actinin along the cell margins appear larger and more irregularly shaped than those in the interior of the cell.

The distribution of anti-α-actinin staining was analyzed from several kinds of images. Our initial observations were all based on fluorescence photomicrographs taken at a single focal plane. Such images contain information regarding the x and y position of all structures with high resolution, but, as pointed out previously, with 1/10 the resolution along the Z-axis. In order to improve the resolution along the Z-axis, we obtained stereo pairs of the fluorescence distribution by two different techniques. First, we obtained stereo-pair fluorescence photomicrographs using a half-aperture near the rear focal plane of the objective. While this technique allows one to obtain information regarding the Z-axis position of stained elements within the depth of field of the objective, the introduction of the half-aperture decreases the resolving power of the lens. Additionally, this technique allows only the assessment of the distribution of fluorescently stained elements in a 2.0-μm deep portion of the cell at a time. An alternative approach has been developed which utilizes the full resolving power of the objective lens in the x, y-plane and allows for assessment of the Z-axis position of stained structures within the entire depth of the cell. While this approach has yielded the most complete representation of the three-dimensional distribution of anti-α-actinin staining in a single cell, further development of this technique should yield even more detailed information. The principal limitation to the present approach is that stained elements are

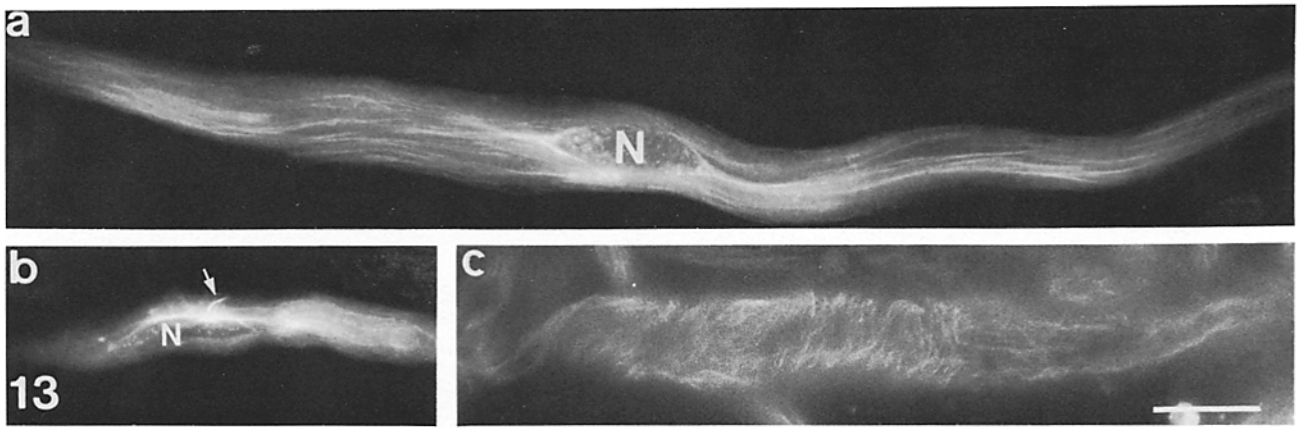

FIGURE 13 Three smooth muscle cells stained with antitubulin. The cells in *a* and *b* were fixed while relaxed and that in *c* was fixed while contracted. The microtubules in the relaxed cell run parallel to the long axis of the cell. The micrograph shown in *a* was obtained with the focal plane midway through the nucleus. Note that the microtubules appear almost to cradle the nucleus (*N*), and that a punctate antitubulin staining pattern is observed within the nucleus itself. In *b*, the microscope was focused at the cell center from which microtubules running parallel to the long axis of the cell appear to emanate. Note that the primary cilium (arrow), which was seen in all cells stained with antitubulin, runs perpendicular to the long axis of the cell originating from the cell center. In the contracted cell shown in *c*, the microtubules run at steep angles to the long axis of the cell in an undulating pattern.

assigned to only one focal plane within the cell, and thus information regarding the tilt of such elements relative to the plane of focus is lost. Such information would facilitate, for example, tracking of strings of stained elements that follow a course that is not parallel to this plane. While further developments in deblurring techniques may yield more complete insights into the arrangement of α-actinin-containing structures within the smooth muscle cell, the present studies have provided us with new and significant information.

In relaxed smooth muscle cells internal structures stained by anti-α-actinin were often seen to exist in what appears to be a stringlike array. Stereo pairs obtained by the method of Osborn et al. (22) as well as computer reconstructions clearly show that these stringlike arrays run within the interior portions of the cell and are not detectable only in the region adjacent to the cell membrane as reported by Bagby (2). These linear arrays, while detectable throughout the entire length of the cell, are most easily visualized in the regions adjacent to the nucleus where the absence of nuclear staining results in less out-of-focus fluorescence and hence higher contrast. In a number of areas of all relaxed cells, linear arrays of stained elements are observed to head toward a larger stained patch along the cell periphery where it appears to terminate.

These linear arrays most probably constitute a basic contractile element of the smooth muscle cell and the material between successive anti-α-actinin-stained elements an even more basic sarcomerelike unit. Certainly, the apparent termination of these linear elements at the large stained patches along the cell periphery is consistent with this proposal. If indeed these linear arrays are the site for generation of force or active cell shortening, then one would predict that: (*a*) these linear elements must be cohesive and thus be preserved in contracted cells; (*b*) active cell shortening would be associated with a decrease in the distance between successive elements in such linear arrays; (*c*) in both contracted and relaxed cells these linear arrays must terminate on at least two sites on the cell periphery in order that shortening of the units comprising such arrays may cause overall cell shortening. Such linear arrays have been observed in both relaxed and contracted cells, consistent with the proposal that these arrays must be cohesive elements. Measurements on these arrays indicate that in actively shortened cells successive stained elements have moved toward one another, a *sine qua non* if these arrays are to be considered contractile elements. Comparison between the course of these linear arrays with that of microtubules in relaxed and contracted cells suggests that the decrease in spacing between stained elements in these linear arrays can not be simply explained as resulting from general compressive forces operating on all cytoplasmic structures. Instead, it is quite likely that these linear arrays are themselves capable of shortening and thus responsible for the observed active contraction. As pointed out above, for such linear arrays to be responsible for contraction of the smooth muscle cell they must be attached at least at two points to the cell surface. To date, we have observed regions of the cell where a linear array appears to terminate at one of the large anti-α-actinin-stained plaques along the cell periphery. However, we have not yet been able to successfully track the other end of such linear arrays to another point of termination. This may well be a consequence of the fact that even our most complete three-dimensional reconstructions have only been attempted for ~25% of the cell length and thus the other point of termination may have been deleted. It is, of course, also possible that continuity of these arrays between points of termination may involve branching, a possibility that might be investigated when more complete three-dimensional reconstructions become available.

If, as is suggested above, contraction of the linear arrays of anti-α-actinin is responsible for cell shortening, it is appropriate to inquire what geometrical constraints must be incorporated into schemes for the distribution of actin and myosin within such elements. Bond et al. (4) have presented data indicating that oppositely directed actin filaments emerge from either end of cytoplasmic dense bodies. Thus, the material contained between a pair of cytoplasmic dense bodies or anti-α-actinin stained elements may well represent a sarcomerelike unit. If that is the case, then myosin filaments must be positioned within the cell so that they can interact with such oppositely directed actin filaments in order to produce cell shortening. Ashton et al. (1) have carefully studied the dimensions of thick filaments in rat mesenteric portal veins, finding a mean length of 2.2 μm. While similar detailed data are not available for

smooth muscle cells of the stomach muscularis of *Bufo marinus*, preliminary data on relaxed isolated smooth muscle cells from this tissue suggest that thick filaments are comparable in length to those in mammalian species. It is thus unlikely from dimensional considerations that the myosin filaments would be disposed between two successive anti-α-actinin-stained elements even in relaxed smooth muscle cells. While the distance between midpoints of successive anti-α-actinin-stained elements is 2.2 μm on the average, each of these stained elements is at least 1.0 μm long, leaving little more than a 1-μm space between successive stained elements for a myosin filament that is probably considerably longer than 1.0 μm. It thus seems more likely that myosin filaments are positioned peripheral to individual linear arrays interacting with oppositely directed actin emerging from cytoplasmic dense bodies that are arranged in this linear manner. Further insights into this interrelation must await high resolution observations of anti-α-actinin and anti-myosin staining in both fixed and living smooth muscle cells.

Our data indicate that several of these strings often run in parallel for some distance with elements in neighboring strings in lateral register. It thus appears in some regions of the cell that linear arrays are incorporated into a matlike contractile structure. The integrity of this structure appears to be maintained during the movement of cellular elements that accompanies contraction. This raises the possibility that the linear arrays are held together and in lateral register by some fixed structure. A similar lateral registration of Z-disks is known to occur in striated muscle, where the regions between in register Z-disks contain a high density of intermediate filaments. These arrays of intermediate filaments have been hypothesized as being responsible for the observed registration (21). It is tempting to speculate that a similar structure may exist within the smooth muscle cell in order to account for the observed registering of anti-α-actinin-stained elements.

In summary, the present studies have revealed that α-actinin is incorporated into numerous discrete elements within the cytoplasm of a smooth muscle cell. These elements appear to be part of the contractile machinery per se. They are organized into stringlike arrays that terminate at larger anti-α-actinin-stained plaques along the cell periphery. Futhermore, several of these stringlike arrays often run in parallel and in close proximity for some distance with the anti-α-actinin-stained elements in adjacent strings in lateral register. These observations suggest that the contractile proteins within smooth muscle may be more extensively organized than previously thought. Further insights into this pattern of organization should be forthcoming from more complete three-dimensional reconstructions of the distribution of α-actinin in conjunction with other proteins involved in the contractile process. These studies promise in turn to greatly enhance our understanding of the structural basis for many of the unique physiological properties of smooth muscle (11).

The authors wish to gratefully acknowledge the advice and assistance of Mr. Peter Ley and Ms. Rosanne Hoffmann with photography, and the help of Mr. Cyril Rodgers in coupling the eddy current sensor to the microscope.

This work was supported in part by grants from the National Institutes of Health (HL 14523; GM 25637; BRSG S07 RR05381) and the Muscular Dystrophy Association of America.

Part of the work described in this paper was presented at the Twenty-first Annual Meeting of the American Society for Cell Biology (9).

Received for publication 21 June 1982, and in revised form 3 November 1982.

REFERENCES

1. Ashton, F. T., A. V. Somlyo, and A. P. Somlyo. 1975. The contractile apparatus of vascular smooth muscle by intermediate high voltage stereo electron microscopy. *J. Mol Biol.* 98:17–29.
2. Bagby, R. M. 1980. Double immunofluorescent staining of isolated smooth muscle cells. I. Preparation of anti-chicken gizzard α-actinin and its use with anti-chicken gizzard myosin for colocalization of α-actinin and myosin in chicken gizzard cells. *Histochemistry* 69:113–129.
3. Bagby, R. M., and F. A. Pepe. 1978. Striated myofibrils in anti-myosin stained isolated chicken gizzard smooth muscle cells. *Histochemistry* 58:219–235.
4. Bond, M., A. V. Somlyo, T. M. Butler, and A. P. Somlyo. 1981. Dense bodies, actin polarity and the state of myosin in vertebrate smooth muscle. VII International Biophysics Congress and III Panamerican Biochemistry Congress.
5. Cooke, P. H., and F. S. Fay. 1972. Thick myofilaments in contracted and relaxed mammalian smooth muscle cells. *Exp. Cell Res.* 71:265–272.
6. Devine, C. E., and A. P. Somlyo. 1971. Thick filaments in vascular smooth muscle. *J. Cell Biol.* 49:636–649.
7. Fay, F. S., P. H. Cooke, and P. G. Canaday. 1976. Contractile properties of single isolated smooth muscle cells. *In* Physiology of Smooth Muscle. E. Bulbring and M. F. Shuba, editors. Raven Press, New York. 249–264.
8. Fay, F. S., and C. M. Delise. 1973. Contraction of isolated smooth muscle cells-structural changes. *Proc. Natl. Acad. Sci. USA.* 70:641–645.
9. Fay, F. S., and K. Fujiwara. 1981. Organization of α-actinin in relaxed and contracted single isolated smooth muscle cells. *J. Cell Biol.* 91:358a. (Abstr.)
10. Fay, F. S., R. Hoffman, S. LeClair, and P. Merriam. 1982. Preparation of individual smooth muscle cells from the stomach of *Bufo marinus*. *Methods Enzymol.* 85B:284–291.
11. Fay, F. S., D. D. Rees, and D. M. Warshaw. 1981. The contractile mechanism in smooth muscle. *In* Membrane Structure and Function. Vol. 4. E. E. Bittar, editor. John Wiley and Sons, New York. 79–130.
12. Fay, F. S., and J. J. Singer. 1977. Characteristics of response of isolated smooth muscle cells to cholinergic drugs. *Am. J. Physiol.* 232:C144–C154.
13. Fujiwara, K., and T. Pollard. 1978. Simultaneous localization of myosin and tubulin in human tissue cultured cells by double antibody staining. *J. Cell Biol.* 77:182–194.
14. Fujiwara, K., M. R. Porter, and T. D. Pollard. 1978. Alpha-actinin localization in the cleavage furrow during cytokinesis. *J. Cell Biol.* 79:268–275.
15. Fisher, B. A., and R. M. Bagby. 1977. Reorientation of myofilaments during contraction of a vertebrate smooth muscle. *Am. J. Physiol.* 232:C5–C14.
16. Gabella, G. 1981. Structure of smooth muscles. *In* Smooth Muscle: An Assessment of Current Knowledge. E. Bulbring, A. F. Brading, A. W. Jones, and T. Tomita, editors. University of Texas Press, Austin, TX. 1–46.
17. Goll, D. E., A. Suzuki, J. Temple, and G. R. Holmes. 1972. Studies on purified α-actinin. I. Effect of temperature and tropomyosin on α-actinin/F-actin interaction. *J. Mol. Biol.* 67:469–488.
18. Groschel-Stewart, U., J. H. Chamley, G. R. Campbell, and G. Burnstock. 1975. Changes in myosin distribution in dedifferentiating smooth muscle cells in tissue culture. *Cell Tiss. Res.* 165:13–22.
19. Groschel-Stewart, U., J. A. Chamley, J. D. McConnel, and G. Burnstock. 1975. Comparison of the reaction of cultured smooth and cardiac muscle cells and fibroblasts to specific antibodies to myosin. *Histochemistry* 43:215–224.
20. Laemmli, U. K. 1970. Cleavage of structural proteins during the assembly of the head of bacteriophage T_4. *Nature (Lond.).* 227:680–685.
21. Lazarides, E. 1980. Intermediate filaments—mechanical integrations of cellular space. *Nature (Lond.).* 283:249–256.
22. Osborn, M., T. Born, H. J. Kotsch, and K. Weber. 1978. Stereo immunofluorescence microscopy. I. 3-Dimensional arrangement of microfilaments, microtubules and tonofilaments. *Cell.* 14:477–488.
23. Pease, D. C., and S. Molinari. 1960. Electron microscopy of muscular arteries; pial vessels of the cat and monkey. *J. Ultrastruct. Res.* 3:447–468.
24. Rees, D. D., and F. S. Fay. 1982. Preparation and characterization of fluorochrome-labelled toad stomach α-actinin. *Biophys. J.* 37:54a. (Abstr.)
25. Rice, R. V., J. A. Moses, G. M. McManus, A. C. Brady, and L. M. Blasik. 1970. The organization of contractile filaments in a mammalian smooth muscle. *J. Cell. Biol.* 47:183–196.
26. Schollmeyer, J. E., L. J. Furcht, D. E. Goll, R. M. Robson, and M. H. Stromer. 1976. Localization of contractile proteins in smooth muscle cells and in normal and transformed fibroblasts. *In Cell Motility*, Book A. R. Goldman, T. Pollard, and J. Rosenbaum, editors. Cold Spring Harbor Laboratory, New York. 361–388.
27. Small, J. V. 1974. Contractile unit in vertebrate smooth muscle cells. *Nature (Lond.).* 249:324–327.
28. Small, J. V. 1977. Studies on isolated smooth muscle cells: the contractile apparatus. *J. Cell. Sci.* 24:327–349.
29. Sorokin, S. 1962. Centrioles and the formation of rudimentary cilia by fibroblasts and smooth muscle cells. *J. Cell Biol.* 15:363–377.
30. Suzuki, A., D. E. Goll, I. Singh, R. E. Allen, R. M. Robson, and M. H. Stromer. 1976. Some properties of purified skeletal muscle α-actinin. *J. Biol. Chem.* 251:6860–6870.
31. Tucker, R. W., A. B. Pardee, and K. Fujiwara. 1979. Centriole ciliation is related to quiescence and DNA synthesis in 3T3 cells. *Cell.* 17:527–535.